PCCP

PAPER

Cite this: *Phys. Chem. Chem. Phys.*, 2014, **16**, 16547

Determining the molecular basis for the pH-dependent interaction between 2′-deoxynucleotides and 9*H*-pyrido[3,4-*b*]indole in its ground and electronic excited states†

M. Micaela Gonzalez,[ab] M. Paula Denofrio,[b] Fernando S. García Einschlag,[c] Carlos A. Franca,[d] Reinaldo Pis Diez,[d] Rosa Erra-Balsells*[a] and Franco M. Cabrerizo*[b]

Received 4th May 2014,
Accepted 16th June 2014

DOI: 10.1039/c4cp01910e

www.rsc.org/pccp

Interaction between norharmane and three different 2′-deoxynucleotides (dNMP) (2′-deoxyguanosine 5′-monophosphate (dGMP), 2′-deoxyadenosine 5′-monophosphate (dAMP) and 2′-deoxycytidine 5′-monophosphate (dCMP)), in aqueous solution, was studied in the ground state by means of UV-vis and ^{1}H-NMR spectroscopy and in the first electronic excited state using steady-state and time-resolved fluorescence spectroscopy. In all cases, the norharmane–dNMP interaction dependence on the pH was examined. Possible mechanisms for the interaction of both ground and electronic excited states of norharmane with nucleotides are discussed. Spectroscopic, molecular modeling and chemometric analysis were performed to further characterize the chemical structure of the complexes formed and to get additional information concerning the interaction between dNMPs and norharmane.

Introduction

β-Carbolines (βCs) are a group of efficient naturally occurring photosensitizers. Upon UVA excitation, these alkaloids induce damage in the DNA moiety[1–5] and its components.[6] Briefly, the type and extent of the DNA damage strongly depend on the chemical nature of the βC and also on their binding affinity. Moreover, the latter is modulated by the pH: the lower the pH, the higher the affinity of the βCs and the biomolecules. Although photo-excited βCs are able to produce reactive oxygen species (ROS), even upon two-photon excitation,[7–9] the DNA photosensitized damage takes place, mainly, through electron transfer processes (type I mechanism).

In the recent decades, interest in the photophysics and photochemistry of βCs in aqueous environments has continuously increased. Thus, their photophysics,[7,9–20] photochemistry[7,8] and their interaction[6,21–23] with several biomolecules have been described. Furthermore, interest in this kind of systems arises not only from their role in biological systems, but also from their possible applications in other fields of studies: *i.e.*, development of organic semiconductor devices like light emitting diodes[24,25] and photovoltaic cells. In such systems, the packing and co-assembly of hetero-aromatic rings play a key role in the efficiency of conduction.[26]

In particular, the interaction of βCs with some nucleotides has been investigated:

(i) Balón *et al.*[21] have studied the interaction between harmane and nucleobases, nucleosides and nucleotides, in methanol–water solutions at pH 8.7. They reported that the interaction between these molecules is mainly due to static interaction (formation of ground-state-complexes between the substrates). The nucleobases would only interact with the neutral form of harmane. The magnitude of the binding constants depends, almost exclusively, on the nature of the nucleobase and neither the ribose nor the phosphate groups significantly contribute to the overall binding. The exact nature of the attractive forces involved in the formation of the complexes could not be clearly characterized. However, the stacking of the hetero-aromatic rings of harmane and the nucleobase in the complexes would play a major role in the stabilization of the complexes. Time-resolved fluorescence measurements indicated that a contribution of both static and dynamic quenching

[a] *CIHIDECAR - CONICET, Departamento de Química Orgánica, Facultad de Ciencias Exactas y Naturales, Universidad de Buenos Aires, Pabellón 2, 3p, Ciudad Universitaria, (1428) Buenos Aires, Argentina. E-mail: erra@qo.fcen.uba.ar*
[b] *IIB-INTECH (sede Chascomús) - UNSAM-CONICET, Intendente Marino Km 8,2. CC 164, (7130) Chascomús, Buenos Aires, Argentina. E-mail: fcabrerizo@intech.gov.ar*
[c] *INIFTA - CONICET, Facultad de Ciencias Exactas, Universidad Nacional de La Plata, CCT La Plata-CONICET. Casilla de Correo 16, Suc. 4, (1900) La Plata, Buenos Aires, Argentina*
[d] *CEQUINOR - CONICET, Facultad de Ciencias Exactas, Universidad Nacional de La Plata, calle 47 y 115, (1900) La Plata, Buenos Aires, Argentina*

† Electronic supplementary information (ESI) available. See DOI: 10.1039/c4cp01910e

components operates in the deactivation of the first singlet excited state (S_1) of the βC. The dynamic component would be the proton transfer between the protonated harmane, in its S_1 state, and the phosphate group of the mononucleotide. However, this hypothesis seems to be unlikely for all the acidic and basic species of the three nucleotides.

It is known that, in aqueous solution, βCs and nucleobases show several acid–base equilibria (Scheme 1).[27] Therefore, under the above pH-conditions (pH 8.7), a mixture of different species of both the βC and the dNMP are present in the solution. Thus, a comprehensive study of the molecular interaction as a function of pH would certainly help to understand the contribution of each species to the overall interaction mechanisms.

(ii) Recently, we have demonstrated that the ground state interaction between norharmane and 2′-deoxyadenosine-5′-monophosphate (dAMP) shows a strong pH-dependence that can be explained in terms of the chemical structure of both molecules.[6] In contrast to what is described in the literature,[21] the highest binding constants were estimated under those pH conditions where the protonated form of the alkaloid is present (pH < 7). Theoretical modeling suggested that, despite the fact that the norharmane molecule interacts with adenosine base by π-stacking, the phosphate group also plays a key role in the relative orientation of the two molecules *via* coulombic interactions and also *via* hydrogen bonding with the βC due to the negative charge density present on it. Fluorescence studies[6] revealed that under acidic conditions (*i.e.*, pH 2.5–5.4, where the protonated form of norharmane, $nHoH^+$, is present) the S_1 of protonated norharmane is deactivated by dAMP *via* a purely static process. On the other hand, in alkaline media (pH 10.5), where the neutral form of norharmane (nHo) is predominant, the quenching involves a combination of dynamic and static processes, showing a relatively high efficiency of S_1 deactivation. Reyman *et al.*[28] have recently suggested that such a dynamic deactivation can be a consequence of a proton exchange between the phosphate group and the βC moiety, yielding the corresponding zwitterionic form of the βC.

Despite the aforementioned results, there are indeed several controversies and queries that still need to be addressed: what is the effect of pH on the interaction between βCs (in both their ground and excited states) and nucleotides? Does the nature of the nucleotide (*i.e.*, purine or pyrimidine) affect the binding affinity and the interaction mode? What is the physical nature of the intermolecular interaction forces involved in such complexes: pure π-stacking, pure electrostatic attraction, hydrogen bonding or mixed contributions? What is the role of the phosphate group, present in the nucleotide moiety, in the interaction mode: stabilizes and/or induces a relative orientation between the two moieties? Do proton-transfer processes take place between the first electronic excited state of βC and nucleotides? Does the phosphate group present in the nucleotide moiety participate in proton-transfer processes yielding the zwitterionic form of βC, as suggested in the literature?[28]

In the present work, we have systematically investigated the interaction between norharmane and different nucleotides in aqueous solutions as a function of pH. Since norharmane represents the common heterocyclic skeleton moiety of full aromatic βCs, its use as a model of βC is a reasonable starting point.[29] As a proof of principle, two nucleotides were selected as ligands: 2′-deoxyguanosine 5′-monophosphate (dGMP) and 2′-deoxycytidine 5′-monophosphate (dCMP), as a model of purine and pyrimidine nucleobases, respectively. Results obtained herein were analyzed in connection with those previously reported for dAMP. Molecular modeling and chemometric analysis were also performed to further characterize the chemical structure of the complexes formed and to get from the UV-absorbance spectra additional information concerning the interaction between dNMPs and norharmane.

Experimental methods

Chemicals

Norharmane (>98%), 2′-deoxynucleotides (dNMP: 2′-deoxyguanosine 5′-monophosphate (dGMP), 2′-deoxyadenosine 5′-monophosphate (dAMP) and 2′-deoxycytidine 5′-monophosphate (dCMP)) and other chemicals were provided by Sigma-Aldrich and used without further purification. The pH of the aqueous solutions was adjusted by adding drops of HCl or NaOH solutions (concentrations ranged from 0.1 M to 2 M) from a micropipette. In the experiments performed with D_2O as solvent, D_2O (>99.9%; Euriso-top or Aldrich), deuterium chloride (35 wt% solution in D_2O, 99 atom% D, Aldrich), and sodium deuteroxide (40 wt% solution in D_2O, 99+ atom% D, Aldrich) were employed.

pH measurements were performed with an Altronix TPX-III pH-meter, using a Silver Cap (U.S.A.)-ALPHA PY41 pH-electrode. The pD values were calculated by adding 0.4 to the pH values measured.[30]

Binding studies

The interaction between norharmane and 2′-deoxynucleotides (dNMP) was studied under three pH conditions in which there exists predominantly one acidic–basic form of both norharmane and each nucleotide (*i.e.*, pH 2.8, 5.5 and 10.5 for dCMP and 5.0, 8.5 and 10.5 for dGMP). Previously published results[6] obtained for the norharmane–dAMP systems are also included for comparative purposes. Three different techniques were used to explore the interaction:

(a) UV-vis spectrophotometric titration. Details of the system and the method used have been described elsewhere.[32] Briefly, the spectra were recorded on a Perkin Elmer lambda 25 spectrophotometer. Measurements were made in quartz cells of 1 cm optical-path length, at room temperature. The concentration of norharmane aqueous solutions varied depending on the interaction studied (see footnotes in the corresponding figures) and dNMP concentrations varied from 0 to 50 mM. Experimental difference (ED) spectra were obtained by subtracting the spectrum of dNMP at 0 mM from the subsequent spectra recorded at different dNMP concentrations.

(a.1) Benesi–Hildebrand analysis. Assuming a 1 : 1 stoichiometry for the ground state complexes formed between norharmane

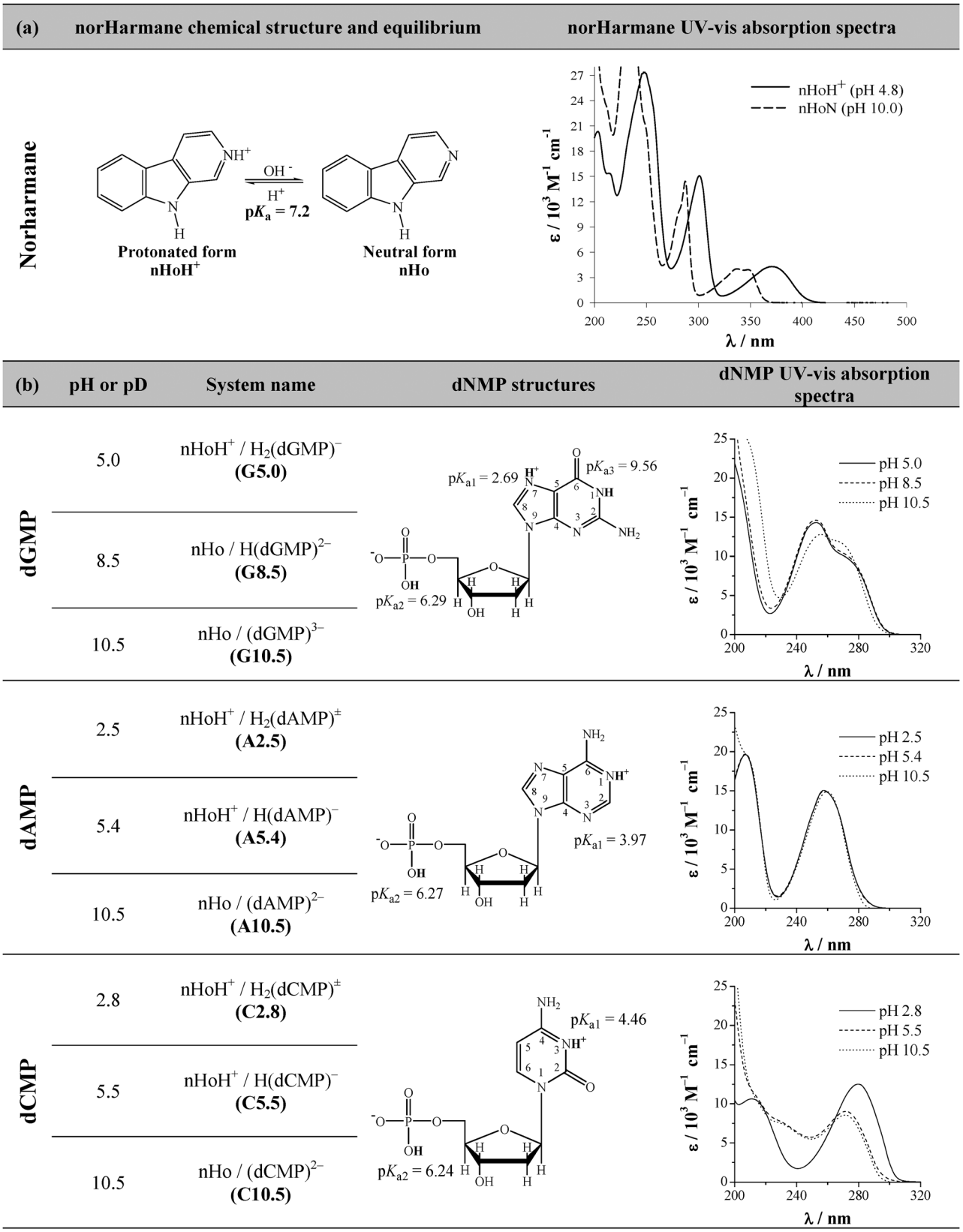

Scheme 1 (a) Molecular structure and UV-vis absorption spectra of the protonated and neutral species of norharmane recorded in air-equilibrated aqueous solutions. The nitrogen of the indolic ring of norharmane has a $pK_a > 13$. (b) Norharmane and dNMP systems present under each pH condition investigated in this work, chemical structures and UV-vis spectra of dNMPs as a function of pH.

and dNMP, the association constants (K_{G1}) were estimated by using the Benesi–Hildebrand equation (eqn (1)):

$$\frac{1}{\Delta A} = \frac{1}{(\varepsilon_{nHo\cdot dNMP} - \varepsilon_{nHo})}\frac{1}{[nHo]_o} + \frac{1}{K_{G1}(\varepsilon_{nHo\cdot dNMP} - \varepsilon_{nHo})[nHo]_o}\frac{1}{[dNMP]} \quad (1)$$

where $\varepsilon_{nHo\cdot dNMP}$ and ε_{nHo} are the molar absorption coefficients of the norharmane·dNMP complex and nHo, respectively, at the titration wavelength. ΔA is the change of absorbance, at a concentration of dNMP, relative to the completely free norharmane ([dNMP] = 0 M) at the same wavelength. K_{G1} values were obtained from the slopes and intercepts of eqn (1).

(a.2) Chemometric analysis. We used curve resolution techniques[31] in order to retrieve, from the absorbance matrix, relevant information concerning the interaction between dNMP and norharmane.[32,33] Bilinear methods can provide information about composition changes in an evolving system; therefore we applied the alternating least-squares (ALS) algorithm to simultaneously estimate concentration and spectral profiles.[34] The ALS method is capable of extracting useful information from the experimental absorbance matrix $\mathbf{A}(i \times j)$ by the iterative application of the matrix product $\mathbf{A} = \mathbf{CS}^{\mathbf{T}} + \mathbf{E}$, where $\mathbf{C}(i \times n)$ is the matrix of the concentration profiles, $\mathbf{S}^{\mathbf{T}}(n \times j)$ is the matrix of the spectral profiles, and $\mathbf{E}(i \times j)$ represents the error matrix. The indexes i, n, and j denote the sample number, absorbing species, and recorded wavelengths, respectively. Retrieving matrices **C** and **E** from matrix **A** may be a rather difficult task[35] since, on the one hand, n is usually unknown,[36] and on the other hand, curve resolution methods cannot deliver a single solution because of rotational and scale ambiguities.[37] We applied singular value decomposition (SVD) of **A** for the estimation of n. In addition, some chemically relevant constraints,[38] such as non-negativity, unimodality and closure, were imposed during the iterative steps of constrained linear regression in order to reduce rotational ambiguities. In addition, the matrix augmentation strategy[39] was used to obtain (i) the number of species required to reproduce the spectral behavior within the entire range of pH studied, (ii) the concentration profiles corresponding to experiments performed using different pH values, and (iii) the spectra of the ground-state complexes formed between norharmane and dNMP.

(b) Fluorescence measurements. The experimental setup has been described elsewhere.[6] Briefly, fluorescence measurements were performed using a single photon counting setup (FL3 TCSPC-SP, Horiba Jobin Yvon) using a FluoroHub-B timing electronic device, in 0.4 × 1 cm path length quartz cells, at room temperature. (i) Steady-state measurements: corrected fluorescence spectra of norharmane were recorded in the presence and in the absence of dNMPs. Experiments were carried out using aqueous solutions of norharmane (~20 μM) and different concentrations of nucleotides (see below). The fluorescence intensity, I_F, was obtained by integration of the corrected fluorescence spectra over the entire emission profile. (ii) Time-resolved measurements: the same set of solutions as mentioned above was analyzed by time correlated fluorescence. A NanoLED source centered at 341 nm was used for excitation, whereas emission decays were monitored at 450 nm. Under our experimental conditions, all the fluorescence lifetimes, τ_F, were obtained from mono-exponential decays observed after deconvolution from the instrument response function signal.[40]

Data obtained from steady-state and time-resolved measurements were analyzed according to the Stern–Volmer correlation (eqn (2) and (3), respectively):

$$I_F^0/I_F = 1 + K_{SV}[Q] \quad (2)$$

$$\tau_F^0/\tau_F = 1 + K_D[Q] = 1 + k_q\tau_F^0[Q] \quad (3)$$

where I_F^0 and I_F are the integrated fluorescence intensities and τ_F^0 and τ_F (s) the fluorescence lifetimes in the absence and in the presence of quencher, respectively, k_q is the bimolecular quenching rate constant (L mol^{-1} s^{-1}), [Q] is the quencher concentration (mol L^{-1}), and K_{SV} and K_D are the Stern–Volmer constant (L mol^{-1}) and the constant for the dynamic quenching, respectively.

The former analysis is a reliable method for differentiating between static and dynamic quenching. For instance, if I_F^0/I_F *vs.* [Q] and τ_F^0/τ_F *vs.* [Q] are linear, and have the same slope ($K_{SV} = K_D$), a purely dynamic process can be assumed. In contrast, if a pure static quenching process is operating, I_F^0/I_F increases linearity with [Q] (eqn (2)), whereas eqn (3) is reduced to $\tau_F^0/\tau_F = 1$. In this case, K_{SV} is equal to the equilibrium constant for ground state complex formation (K_{SS}). If both dynamic and static quenching processes are operating, a quadratic plot is observed for I_F^0/I_F *vs.* [Q]. This behavior is mathematically expressed by eqn (4):

$$I_F^0/I_F = (1 + K_D[Q])(1 + K_{SS}[Q]) \quad (4)$$

where K_D and K_{SS} are the K_{SV} values for the dynamic and static quenching, respectively. K_D is equal to $k_q\tau_F^0$ and K_{SS} is the equilibrium constant for complex formation.

(c) Proton nuclear magnetic resonance (^{1}H-NMR). 500 MHz ^{1}H NMR spectra were recorded on a Bruker AM-500 spectrometer, using D_2O as a solvent. The general approach used to quantify the critical aggregation concentration (c.a.c.), the number of molecules per aggregate (n) and the self-association constants ($K_{s\text{-}a}$) has been described previously.[6]

The binding constants between norharmane and dNMP (K_{G2}) were calculated by standard regression analysis using the NMR 1 : 1 binding isotherm (eqn (5)) for fast exchange systems, to fit experimental data:

$$\Delta = \Delta_o C_M^{free}/(1/K_{G2} + C_M^{free}) \quad (5)$$

where Δ is the change in the chemical shift of norharmane ($= \delta_{obs}^{nHo} - \delta_m^{nHo}$), Δ_o is the limiting value when norharmane is fully complexed ($= \delta_{aggr}^{nHo} - \delta_m^{nHo}$) and C_M^{free} is free dNMP concentration, obtained from the analytical dNMP concentration corrected by[41,42]

$$C_M^{free} = C_M - C_L\Delta/\Delta_o \quad (6)$$

where C_M and C_L are the analytical concentrations of dNMP and norharmane, respectively.

It is worth mentioning that, for evaluation of K_{G2}, the initial concentration of each molecule was kept below the c.a.c. determined herein. Briefly, a solution of norharmane was titrated with a concentrated solution of dNMP and the corresponding

^{1}H-NMR spectra were recorded under three different pH conditions (see Scheme 1). Taking into account the corresponding $K_{s\text{-}a}$ and n values, as well as the range of dNMP used, it can be shown that the fraction of self-associated dNMP was below 5%, for all the experimental conditions studied. Therefore, although dNMP concentrations higher than c.a.c. were used, the self-association can be neglected.

Computational methods

Conformational search of norharmane–dNMP complexes. A very large number of conformers both for protonated and neutral forms of norharmane and for the dNMP molecules were explored. The complexes that could be formed by those compounds at different pH were also explored (Fig. 7). Starting geometries of complexes were constructed considering the form the isolated molecules adopt at the corresponding pH. We applied genetic algorithms as implemented in the Balloon program[43] to obtain a set of starting geometries. These geometries were further optimized using the PM6-DH+ method available in the MOPAC software package.[44] Optimizations were done taking into account solvent effects (water) through a polarizable continuum method. For each system under study, the reported heat of formation (HOF) was calculated as an average over those conformations within 2 kcal mol^{-1} from the most stable conformer according to a Maxwell–Boltzmann distribution at 298 K.

Results and discussion

In aqueous media, in the pH range 2–12, norharmane shows an acid–base equilibrium that involves the nitrogen atom of the pyridine ring with a pK_a of 7.2,[18] with a very distinctive UV-vis absorption spectrum of each acid–base form (Scheme 1). The changes in the electronic ground state distribution of this alkaloid have substantial consequences on its photochemical and photophysical properties.[7–9,45] On the other hand, 2′-deoxynucleotides (dNMPs) show several acid–base equilibria involving both the phosphate group and the nucleobases. However, only the protonation/deprotonation of the nucleobases can lead to noticeable consequences in the UV-vis absorption spectra: in the case of $(dGMP)^{3-}$ (pH 10.5) and $H_2(dCMP)^{\pm}$ (pH 2.8), with a net charge on the nucleobase of −1 and +1, respectively, a bathochromic effect was observed (Scheme 1). In contrast, $H_2(dAMP)^{\pm}$ (pH 2.5) shows no shift in its UV-vis absorption spectrum with respect to the uncharged nucleobase, suggesting that the +1 charge is localized in the $N-1$ atom.

To further evaluate the interaction between each acid–base species, experiments were performed under three different pH conditions (Scheme 1), where only a given species of each analyte were present in the solution.

Molecular interaction between norharmane and dNMPs: spectroscopic studies

In order to examine norharmane–dNMPs interaction and its pH-dependence, UV-vis absorption, ^{1}H-NMR and fluorescence spectroscopy were performed:

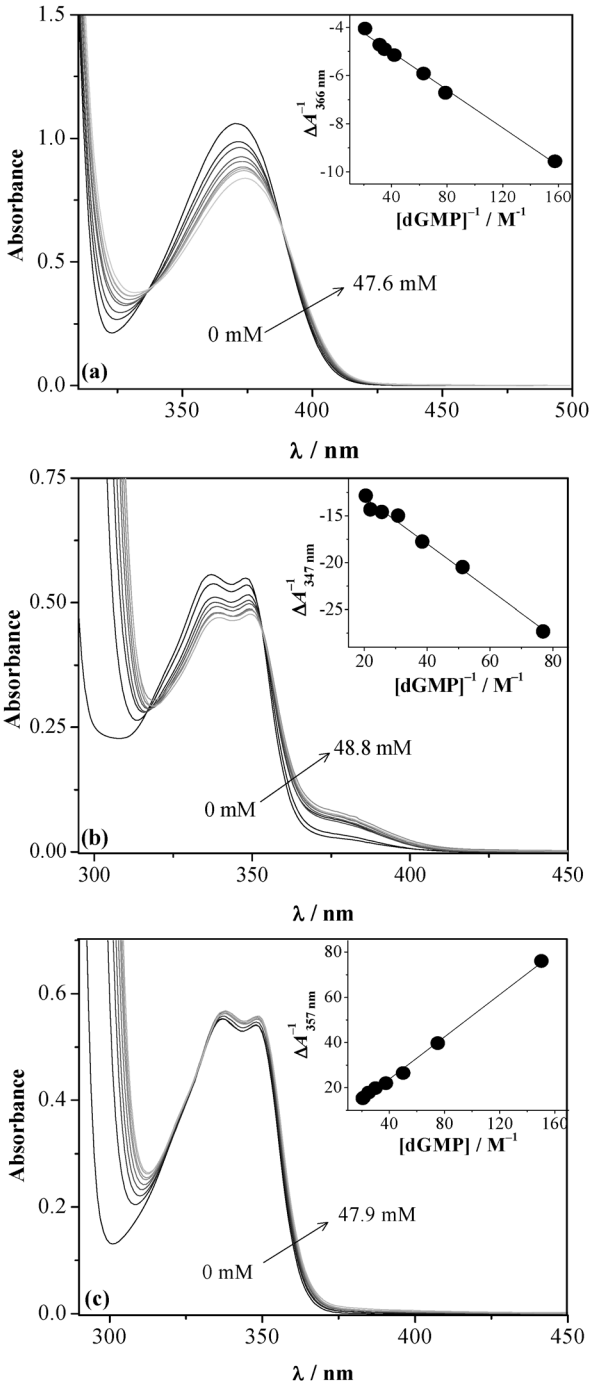

Fig. 1 UV-vis absorption spectra of norharmane (nHo) in the presence of increasing amounts of dGMP (see arrows): (a) $[nHo]_0$ = 250 μM and pH 5.0, (b) $[nHo]_0$ = 150 μM and pH 8.5 and (c) $[nHo]_0$ = 150 μM and pH 10.5. Insets: representatives Benesi–Hildebrand plots.

UV-vis absorption spectroscopy. UV-vis spectra of norharmane aqueous solutions were recorded in the presence of increasing amounts of dNMPs. Fig. 1 shows, as a representative example, results obtained for the norharmane–dGMP system observed at the three pH investigated: G5.0, G8.5 and G10.5. See ESI† for data on the nHo–dCMP system (Fig. S1). Despite that in some cases the recorded changes were small, a clear pH-dependence of each

Table 1 Binding constants (K_{G1} and K_{G2}) between norharmane and dGMP and Stern–Volmer constants for static and dynamic quenching of fluorescence of norharmane by dGMP (K_{SS} and K_D, respectively)

			pH or pD 5.0 G5.0	pH or pD 8.5 G8.5	pH or pD 10.5 G10.5
UV-vis		K_{G1} [a]/M^{-1}	89 ± 2	48 ± 12	11 ± 1
		λ_{iso} [b]/nm	338 and 388	318 and 353	nd
^{1}H-NMR		K_{G2} [c]/M^{-1}	60 ± 10	32 ± 8	21 ± 5
		$K_{s\text{-}a}^{dGMP}$ [c,d]/M^{-1}	0.9 ± 0.2	1.2 ± 0.1	1.0 ± 0.4
		c.a.c.[c]/10^{-3} M	14 ± 1	13 ± 2	14 ± 2
		n[c]	1.8–2	1.9–2	1.6–2
Emission	SS	K_{SS} [e]/M^{-1}	103 ± 2	34 ± 2	25 ± 3[h]
	TR	K_D [e]/M^{-1}	112 ± 2	160 ± 2	188 ± 3
		k_q [f,g]/10^9 L mol^{-1} s^{-1}	5.1 ± 0.2	7.3 ± 0.2	9.0 ± 0.3

[a] Data obtained from UV-vis spectroscopy analysis (eqn (1)). [b] λ_{iso} (nm) is the wavelength of the isosbestic points observed in UV-vis spectra. [c] Data obtained from ^{1}H-NMR spectroscopy analysis. Data listed herein represent the average of the values derived from ^{1}H-NMR analysis of different protons. [d] K_{aa} value of 1.29 M^{-1} has been previously reported[48] for guanosine-5′-monophosphate (5′-GMP), measured at 30 °C and pD 7.4. [e] Values obtained from steady-state, SS, and time-resolved, TR, measurements. In SS experiments, samples were irradiated (λ_{exc}) at wavelengths corresponding to the maximum of absorption of the lowest energy band (Fig. 1), whereas in TR experiments λ_{exc} = 341 nm and λ_{exc} = 450 nm. [f] Bimolecular rate constants for the quenching of the fluorescence of norharmane by the nucleotide. [g] Norharmane fluorescence lifetime used for k_q calculation was 22 ns for both protonated and neutral species of norharmane. The k_q value reported[21] for the fluorescence quenching by phosphate anions, measured in NH_3–NH_4Cl pH 8.7 buffer solutions, was 9.7×10^9 M^{-1} s^{-1}. [h] Data obtained from eqn (4), using the K_D value obtained from eqn (3) as a fixed value for iteration. $K_{s\text{-}a}$, n and c.a.c. values for nHoH$^+$ and nHo, at pD 5.0 and 10.5, are (7 ± 1) M^{-1}, 2, (4 ± 1) mM and (80 ± 16) M^{-1}, 2, nd, respectively.

nHo–dNMP interaction was observed. This fact indicates the presence of an interaction between each acid–base species of norharmane and dNMPs in their electronic ground states. In most cases, the absorption spectra showed a moderate bathochromic shift (~5 nm) and the appearance of at least two visible isosbestic points (see λ_{iso} in Tables 1–3). The small bathochromic shift observed suggests that the interaction operates through other kinds of interactions different from hydrogen bonding (see below).

As a general trend, increasing concentrations of dNMP lead to a decrease in the intensity (hypochromic effect) of the lowest energetic absorption band maxima of norharmane (Fig. 1 and Fig. S1 in ESI†). Noteworthily, purine deoxynucleotides (dAMP[6] and dGMP) showed higher hypochromic effect than dCMP, a pyrimidine deoxynucleotide. This behavior suggests that, for almost all the pH conditions investigated, non-covalent dispersion interaction (from now on, π-stacking)[46] between the two heteroaromatic rings contributes, among other intermolecular forces, to the overall interaction between norharmane and dNMP. System C2.8 constitutes an exception to this behavior: the intensity of the absorption spectra decreases with increasing nucleotide concentration, without the appearance of either bathochromic effect or isosbestic points (Fig. S1a in ESI†). In this case, the electrostatic repulsion between the two positive net charges, placed in both the norharmane and the cytosine rings, would explain the distinctive behavior (see below). This fact is in good agreement with

Table 2 For a comparative purpose, data corresponding to norharmane–dAMP systems, already published,[6] are listed herein. Binding constants (K_{G1} and K_{G2}) between norharmane and dAMP and Stern–Volmer constants for static and dynamic quenching of the fluorescence of norharmane by dAMP (K_{SS} and K_D, respectively)[47]

			pH or pD 2.5 A2.5	pH or pD 5.4 A5.4	pH or pD 10.5 A10.5
UV-vis		K_{G1} [a]/M^{-1}	22 ± 6	64 ± 8	39 ± 8
		λ_{iso} [b]/nm	328 and 388	328 and 383	307 and 353
^{1}H-NMR		K_{G2} [c]/M^{-1}	13 ± 3	75 ± 9	26 ± 5
		$K_{s\text{-}a}^{dAMP}$ [c,d]/M^{-1}	2 ± 1	2.6 ± 0.9	0.36 ± 0.04
		c.a.c.[c]/10^{-3} M	6.7 ± 0.7	11 ± 2	15 ± 2
		n[c]	1.5–2	1.9–2	1.9–2
Emission	SS	K_{SS} [e]/M^{-1}	17 ± 1	54 ± 7	22 ± 2[h]
	TR	K_D [e]/M^{-1}	0	0	139 ± 3
		k_q [f,g]/10^9 L mol^{-1} s^{-1}	—	—	6.7 ± 0.2

[a] Data obtained from UV-vis spectroscopy analysis (eqn (1)). [b] λ_{iso} (nm) is the wavelength of the isosbestic points observed in UV-vis spectra. [c] Data obtained from ^{1}H-NMR spectroscopy analysis. Data listed herein represent the average of the values derived from ^{1}H-NMR analysis of different protons. [d] $K_{s\text{-}a}$ (in M^{-1}) values of 2.1 ± 0.6, 3.4 ± 0.3 and 2.1 ± 0.3 have been previously reported[49] for adenosine-5′-monophosphate (5′-AMP), measured at pD 3.44, pD 5.61 and pD 8.90, respectively. [e] Values obtained from steady-state, SS, and time-resolved, TR, measurements. In SS experiments, samples were irradiated (λ_{exc}) at wavelengths corresponding to the maximum of absorption of the lowest energy band (Fig. 1), whereas in TR experiments λ_{exc} = 341 nm and λ_{exc} = 450 nm. [f] Bimolecular rate constants for the quenching of the fluorescence of norharmane by the nucleotide. [g] Norharmane fluorescence lifetime used for k_q calculation was 22 ns for both protonated and neutral species of norharmane. The k_q value reported[21] for the fluorescence quenching by phosphate anions, measured in NH_3–NH_4Cl pH 8.7 buffer solutions, was 9.7×10^9 M^{-1} s^{-1}. [h] Data obtained from eqn (4), using the K_D value obtained from eqn (3) as a fixed value for iteration. $K_{s\text{-}a}$, n and c.a.c. values for nHoH$^+$ and nHo, at pD 5.0 and 10.5, are (7 ± 1) M^{-1}, 2, (4 ± 1) mM and (80 ± 16) M^{-1}, 2, nd, respectively.

Table 3 Binding constants (K_{G1} and K_{G2}) between norharmane and dCMP and Stern–Volmer constants for static and dynamic quenching of the fluorescence of norharmane by dCMP (K_{SS} and K_D, respectively)

			pH or pD 2.8 C2.8	pH or pD 5.5 C5.5	pH or pD 10.5 C10.5
UV-vis		K_{G1} [a]/M^{-1}	2.7 ± 0.5	3 ± 2	12 ± 5
		λ_{iso} [b]/nm	None	322 and 379	nd
^{1}H-NMR		K_{G2} [c]/M^{-1}	nd[d]	nd[d]	nd[d]
		$K_{s\text{-}a}^{dCMP}$ [c]/M^{-1}	0.2 ± 0.04	1.1 ± 0.5	1.2 ± 0.7
		c.a.c.[c]/10^{-3} M	22 ± 3	12 ± 1	15 ± 1
		n[c]	1.7–2	1.6–2	1.9–2
Emission	SS	K_{SS} [e]/M^{-1}	3 ± 2	5 ± 1	0
	TR	K_D [e]/M^{-1}	9.3 ± 0.1	12.8 ± 0.2	117 ± 9
		k_q [f,g]/10^9 L mol^{-1} s^{-1}	0.4 ± 0.01	0.6 ± 0.2	5.6 ± 0.5

[a] Data obtained from UV-vis spectroscopy analysis (eqn (1)). [b] λ_{iso} (nm) is the wavelength of the isosbestic points observed in UV-vis spectra. [c] Data obtained from ^{1}H-NMR spectroscopy analysis. Data listed herein represent the average of the values derived from ^{1}H-NMR analysis of different protons. [d] nd = not detected. Due to the extremely small ^{1}H-NMR chemical shifts observed for the C1–H proton signals of norharmane as a function of dCMP concentration, under the three pH conditions, K_{G2} for the hetero-complexes of this particular nucleotide and norharmane could not be determined. [e] Values obtained from steady-state, SS, and time-resolved, TR, measurements. In SS experiments, samples were irradiated (λ_{exc}) at wavelengths corresponding to the maximum of absorption of the lowest energy band (Fig. 1), whereas in TR experiments λ_{exc} = 341 nm and λ_{exc} = 450 nm. [f] Bimolecular rate constants for the quenching of the fluorescence of norharmane by the nucleotide. [g] Norharmane fluorescence lifetime used for k_q calculation was 22 ns for both protonated and neutral species of norharmane. The k_q value reported[21] for the fluorescence quenching by phosphate anions, measured in NH_3–NH_4Cl pH 8.7 buffer solutions, was 9.7×10^9 M^{-1} s^{-1}. $K_{s\text{-}a}$, n and c.a.c. values for $nHoH^+$ and nHo, at pD 5.0 and 10.5, are (7 ± 1) M^{-1}, 2, (4 ± 1) mM and (80 ± 16) M^{-1}, 2, nd, respectively.

the hypothesis that the hypochromic effect would be related to stacking interaction.

Assuming a 1 : 1 stoichiometry, the corresponding association constants (K_{G1}) were calculated by eqn (1). For all cases, a linear behavior was observed, confirming a 1 : 1 stoichiometry for the complexes formed (insets in Fig. 1 and the right column in Fig. S1 in ESI†). The corresponding values of K_{G1} are reported in Tables 1–3.

Briefly, three major points should be highlighted: (i) purine nucleotides show higher affinity for norharmane than the pyrimidine nucleotide: in the whole pH-range investigated, K_{G1}^{dGMP} and K_{G1}^{dAMP} are at least one order of magnitude higher than K_{G1}^{dCMP}. This is in disagreement with the trend described by Balón *et al.* (G ≫ C > A).[21] (ii) K_{G1} values of purine nucleotides show a clear pH-dependence: the trend observed for dGMP was $K_{G1}^{G5.0} > K_{G1}^{G8.5} > K_{G1}^{G10.5}$, whereas the trend for dAMP was $K_{G1}^{A5.4} > K_{G1}^{A10.5} > K_{G1}^{A2.5}$.[6] In each case, the strength of the interactions is tightly correlated to the chemical nature of the corresponding acid–base species of the involved molecules. This trend can be explained in terms of electrostatic interactions: the strongest interaction takes place when the net charges of norharmane and the nucleotide are +1 and −1, respectively (*i.e.*, systems G5.0, A5.4 and C5.5). This fact suggests that, besides the stacking contribution, coulombic forces would also contribute to the overall interaction process between norharmane and nucleotides. These electrostatic attractions would also contribute to the relative orientations of the interacting molecules in the hetero-complex (see below). (iii) In contrast to what was described by Balón *et al.*,[21] our results show that $nHoH^+$ clearly interacts with the three dNMP investigated.

Chemometric analysis. Experimental absorbance matrices at each pH studied were constructed from the absorbance spectra recorded at different dGMP concentrations and analyzed by curve resolution techniques. The wavelength range selected for the analysis was 315–465 nm, since the contribution of the free forms of dGMP to the recorded absorbance can be considered negligible in this wavelength domain. Singular value decomposition of the absorbance matrices obtained at pH 5.0 and 10.5 yielded, in both cases, two factors. For both pH conditions, the spectra of the complex formed as well as the concentration profiles of free and bound norharmane were obtained by application of the ALS algorithm. The constraints used for the iterative process included equality (*i.e.*, the spectra of the free forms $nHoH^+$ and nHo were fixed since they were already known), non-negativity (*i.e.*, concentrations and absorption coefficients cannot be negative) and unimodality (*i.e.* concentration profiles should decrease for reactants, increase for reaction products, or exhibit a single peak for intermediate species). The absorption coefficients obtained by the ALS method for the bound norharmane forms are compared with those of free norharmane forms in Fig. 2a and b. In addition, the insets of Fig. 2a and b show the fractions of free and bound norharmane against the analytical concentration of dGMP at pH 5.0 and 10.5, respectively. Noteworthily, the concentration profiles obtained for free and bound norharmane yielded binding constants that were in fairly good agreement with the values reported in Table 1 (Table S1 in ESI†).

Singular value decomposition of the experimental absorbance matrix obtained at pH 8.5 yielded 3 independent factors suggesting that, at this pH value, more than two species contribute to the recorded absorbance. Inspection of Fig. 1 shows that, except for the small shoulder observed between 360 and 415 nm, the spectral shapes obtained at pH 8.5 are rather similar to those obtained at pH 10.5. Since for the spectra recorded at pH 5.0 the main absorption changes were found within the aforementioned wavelength domain, the experimental results were jointly analyzed by constructing the augmented data matrix, which included the entire set of spectra recorded at different pH values and dGMP concentrations. Singular value decomposition of the augmented data matrix yielded 4 independent factors, thus suggesting that the overall behavior can be explained in terms of two free norharmane

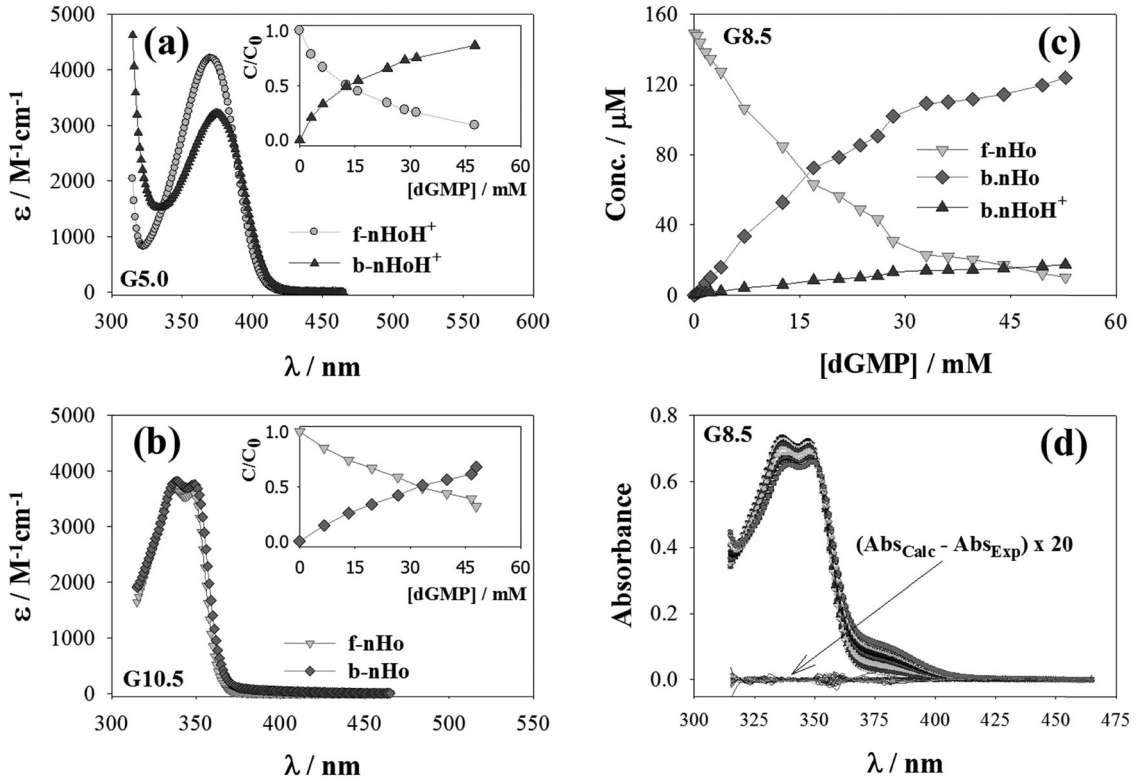

Fig. 2 Results obtained from curve resolution techniques. (a) Absorption spectra of free and bound forms of $nHoH^+$ at pH 5.0. Inset: free and bound fractions of $nHoH^+$ against [dGMP]. (b) Absorption spectra of free and bound forms of nHo at pH 10.5. Inset: free and bound fractions of nHo against [dGMP]. (c) Concentration profiles of free nHo, bound nHo and bound $nHoH^+$ against [dGMP] resolved from the absorbance matrix recorded at pH 8.5. (d) Comparison between the experimental absorbance matrix **A** and the error matrix **E**, calculated as $\mathbf{A} - \mathbf{CS}^T$, at pH 8.5. Free norharmane forms: f-nHo and f-$nHoH^+$; bound norharmane forms: b-nHo and b-$nHoH^+$.

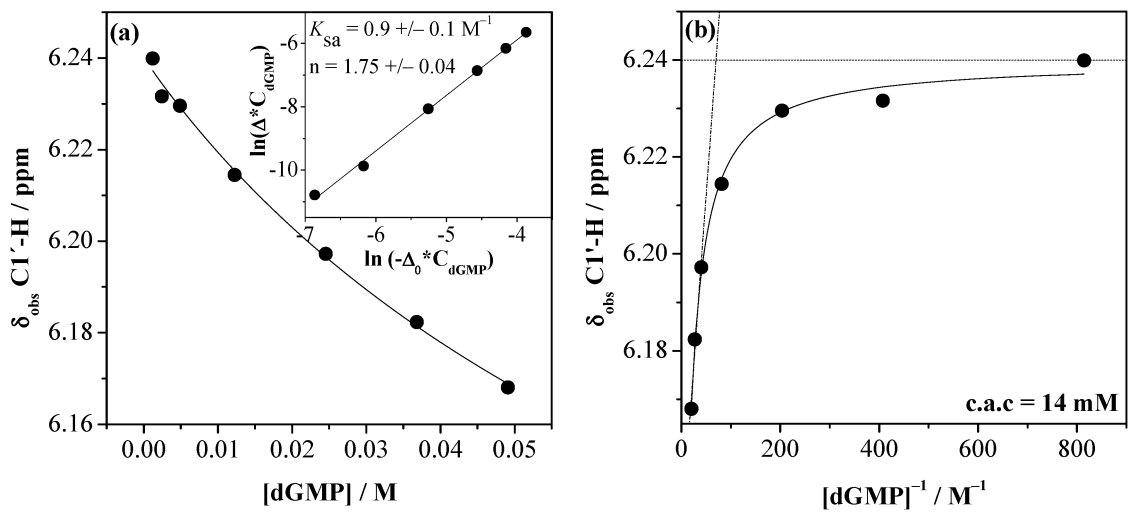

Fig. 3 (a) Chemical shift of C1′–H (δ, in ppm) as a function of $H_2(dGMP)^-$ concentration, measured in D_2O at pD 5.0. Inset: data analysis to obtain the self-association constant, $K_{s-a}^{H_2(dGMP)^-}$, and the number of molecules, n, per aggregate. (b) Critical aggregation concentration (c.a.c.) calculated from the analysis of the chemical shifts of $H_2(dGMP)^-$ C1′–H observed as a function of $[H_2(dGMP)^-]^-$.

forms (f-$nHoH^+$ and f-nHo) and two bound norharmane forms (b-$nHoH^+$ and b-nHo). In order to confirm this hypothesis, we used the spectra shown in Fig. 2a and b to extract, from the absorbance matrix recorded at pH 8.5, the concentration profiles of the four species by means of linear regression. As expected, the results show that as dGMP increases, the fraction of b-nHo increases (Fig. 2c). However, the results also indicate that non-negligible amounts of b-$nHoH^+$ are also formed,

despite that the fraction of f-nHoH$^+$ remains negligible within the experimental error (for simplicity, the profile of f-nHoH$^+$ was omitted from Fig. 2c). Fig. 2d demonstrates that the concentration profiles and the spectra obtained by the chemometric analysis can precisely reproduce the experimental results obtained at pH 8.5. Finally, despite that the experiment was performed at pH 8.5 (*i.e.*, 1.3 pH units above the pK_a of free norharmane), the unforeseen presence of b-nHoH$^+$ may be explained by assuming that complex formation leads to a more pronounced free energy decrease for the protonated than for the deprotonated form of norharmane. Actually, this additional stabilization should result in a shift towards higher pH values of the apparent pK_a for bound norharmane (*i.e.*, pK_a^{app} = 7.5).

The same general trends were obtained for the dAMP–norharmane system (Fig. S2 in ESI†). Additional information concerning the results of the chemometric analysis of norharmane–dGMP and norharmane–dAMP systems is listed in Table S1 of the ESI.† It is worth mentioning that, under the pH condition where a given acid–base species of norharmane (*i.e.*, nHoH$^+$ or nHo) is present, the spectra of the complexes were the same, within the experimental error, for both nucleotides: dGMP and dAMP (Fig. S3 in ESI†). This fact suggests a similar type of interaction between norharmane and these two purine nucleotides and that a π-stacking effect contributes, among other forces (see below), to the overall interaction.

^{1}H-NMR analysis. As described elsewhere,[6] aromatic molecules tend to aggregate in aqueous solution. Thus, the self-association tendency of dNMPs has to be evaluated first. This analysis provides useful information such as the optimal concentrations that can be used in the interaction experiments without the interference of homogeneous multimeric norharmane and/or dNMPs species. Briefly, the changes in the chemical shift of the dNMPs' proton signals were determined for all the acid–base species of dGMP and dCMP as a function of their concentration. The self-association phenomenon for norharmane and dAMP has been previously described.[6]

Fig. 3 shows, as a representative example, the chemical shift of C1′–H proton of $H_2(dGMP)^-$ (pD 5.0). By fitting the experimental results it was possible to accurately obtain the self-association constant, $K_{s\text{-}a}^{H_2(dGMP)^-} = 0.9(\pm 0.2)\ M^{-1}$, as well as the number of molecules per aggregate, n = 1.8–2 (see the inset of Fig. 3a). The latter value suggests that, in the concentration range investigated, $H_2(dGMP)^-$ forms dimeric aggregates. The critical aggregation concentration (c.a.c.) value was also calculated, yielding $14(\pm 1) \times 10^{-3}$ M (Fig. 3b). $K_{s\text{-}a}$, c.a.c. and n values were estimated for all the investigated compounds, under all pH conditions defined in Scheme 1 (Tables 1–3).

From the results collected in Tables 1–3, several points should be highlighted:

• To the best of our knowledge, this is the first time that the self-association constants of each acid–base species of dGMP and dCMP are provided. The values obtained herein substantially agree with those reported in the literature for other related nucleotides.[48,49] In general, these nucleotides show relatively low $K_{s\text{-}a}$ values that are in good agreement with the quite high solubility of these molecules in water. An efficient water-solvation takes place as a consequence of the rather high polarity of the nucleotides due to the presence of phosphate and deoxyribose groups.

• It is generally accepted for these molecules that self-association occurs *via* aromatic-ring stacking of the analytes. However, in a very recent study it was suggested that for relatively small aromatic molecules other types of interaction, apart from π-stacking, can be similarly strong, and thus also important for structure formation.[50] The upfield ^{1}H-NMR shifts, observed in our experiments for all the investigated compounds and pD conditions with increasing dNMP concentration, provide evidence that the stacking of the aromatic moieties is taking place in the self-association interaction mode.

• Although no clear pH-dependence of the $K_{s\text{-}a}^{dNMPs}$ values was observed in the case of dGMP and dCMP, two points deserve to be mentioned: (i) at pD conditions where the phosphate group is completely deprotonated (with a −2 net charge) and the nucleobase is neutral, the corresponding $K_{s\text{-}a}^{dNMPs}$ values were similar for the three nucleotides ($\sim 1\ M^{-1}$). Therefore, under these particular pD conditions, the phosphate group mainly controls the aggregation process. The chemical nature of the nucleobase has no significant effect. In those cases, the nucleotides can be better solvated by the solvent (water), reducing the chance of self-aggregation. (ii) The net charge placed on each nucleobase has different correlation with the aggregation tendency. In the case of $(dGMP)^{3-}$ (at pD 10.5), the $K_{s\text{-}a}^{(dGMP)^{3-}}$ value is the same, within the experimental error, as that observed at pD 5.0 and 8.5. This fact can be explained in terms of a charge delocalization as suggested from the UV-vis absorption spectra shown in Scheme 1. In contrast, $H_2(dCMP)^{\pm}$ (pD 2.8) and $H_2(dAMP)^{\pm}$ (pD 2.5), both with a positive net charge placed on the nucleobase, show a very distinctive behavior: $H_2(dCMP)^{\pm}$ shows the lowest $K_{s\text{-}a}$ value, compared with the self-association constants obtained for the same nucleotide at pD 5.5 and 10.5, whereas $H_2(dAMP)^{\pm}$ shows the highest value, within the experimental error ($K_{s\text{-}a} = 2(\pm 1)\ M^{-1}$). This fact is in agreement with the high and low relative solubility shown by these two species, respectively. Taking into account the stacking contribution to the self-association of the nucleobases, the presence of a positive charge in the nucleobase should decrease the self-association tendency due to electrostatic repulsion forces. However, this is not the general trend. Therefore, our experimental observation should be explained in terms of the stability of each nucleotide conformer. In the most stable conformer observed for $H_2(dAMP)^{\pm}$, the protonated nitrogen of the nucleobase directly interacts with the atoms of oxygen of the sugar ring and/or with the negative charge of the phosphate group, neutralizing the total charge of the zwitterionic species of each nucleotide.[6] Such interaction would lead to an apparent decrease of the nucleotide polarity that would increase the $K_{s\text{-}a}^{H_2(dAMP)^{\pm}}$ value.

• The three dNMP investigated herein, under all pH conditions, have lower self-aggregation tendencies (*i.e.*, lower $K_{s\text{-}a}^{dNMP}$ values) than norharmane. This fact could be a consequence of repulsion forces due to the negative charge present in the phosphate group of dNMP. Moreover, the phosphate group can be better solvated by water, decreasing the self-aggregation tendency. On the other hand,

the low solubility of norharmane is in good accordance with the relatively high $K_{s\text{-}a}$ observed for this alkaloid in aqueous solution.

• For all the cases, under all pD conditions studied, *n* values obtained were ~2, suggesting homo-dimeric aggregation.

The interaction between norharmane and dNMPs was further characterized by ^{1}H-NMR spectroscopy, monitoring the chemical shift deviations of norharmane proton signals upon addition of increasing amounts of dNMPs to a D_2O solution of norharmane (see Experimental section). Except for the system C2.8, the results suggested a contribution of non-covalent π-stacking to the interaction mode (see below the contribution of other intermolecular interaction forces). Fig. 4 shows the chemical shift of C1–H proton of norharmane observed at the three pH values investigated, as a function of dGMP and dCMP concentrations. Results for norharmane–dAMP systems (A2.5, A5.4 and A10.5) were already reported in the literature.[6] The upfield ^{1}H-NMR chemical shifts for the proton signals, together with a slight broadening of the peaks and a significant loss of resolution (Fig. S9a, ESI†), observed as a function of dNMP concentration suggest that the hetero-association occurs, at least partially, *via* stacking of the two aromatic rings.

The C2.8 system represents an interesting exception. In this particular case, downfield ^{1}H-NMR chemical shifts are observed for the proton signals as a function of $H_2(dCMP)^{\pm}$ concentration (see squares in Fig. 4b). Moreover, for this particular case, no changes in the width of the peaks were observed (Fig. S9b, ESI†). These results suggest that the interaction mode for this particular hetero-complex is not π-stacking-like (see below) but most likely *via* hydrogen bonding.

The corresponding binding constants for the hetero-complexes (K_{G2}) were calculated by fitting the experimental data according to eqn (5) and (6) (Tables 1 and 3). These data substantially agree with those obtained from UV-vis titration experiments shown above. In brief, (i) purine nucleotides showed higher affinity to norharmane than dCMP. (ii) The electrostatic attractions between the phosphate group and the protonated pyrimidine nitrogen of norharmane would certainly contribute to the overall affinity, as represented by the highest values observed in G5.0, A5.4 and C5.5 (see above). Moreover, in the case of purine nucleotides, the same pH-trends were observed, since K_{G2} values follow the order $K_{G2}^{(G5.0)} > K_{G2}^{(G8.5)} > K_{G2}^{(G10.5)}$ and $K_{G2}^{(A5.4)} > K_{G2}^{(A10.5)} > K_{G2}^{(A2.5)}$ for dGMP and dAMP[6] systems, respectively. (iii) The hetero-association constants determined herein are, at least, one order of magnitude higher than the corresponding dNMP $K_{s\text{-}a}$ values. Thus, norharmane–dNMP interaction is favored in comparison to the nucleotides' self-association. (iv) Although the corresponding K_{G2} for the hetero-complex formation of dCMP and norharmane could not be determined, from Fig. 4b it is evident that the chemical shifts observed for the C1–H proton signals are smaller than those observed for dGMP and dAMP. This is in agreement with the low hetero-association constants observed for dCMP and norharmane by UV-vis spectroscopy.

Molecular modeling. Theoretical analysis was performed to further investigate the nature of the complexes formed in the electronic ground states. The dispersion- and hydrogen bonding-corrected PM6 method was used to explore the complexes that can be originated from the combination of neutral and protonated forms of norharmane and the three acid–base species of dGMP and dCMP, laying special emphasis on the interaction energy.

In the first place, a conformational search for the three forms of free nucleotides was done. Briefly, $(dGMP)^{3-}$ led to 23 conformations, within the energy penalty of 2 kcal mol^{-1}, most of them in an *anti* conformation (including the most stable one), in which the N9–C8 bond projects onto or near the sugar ring, as usually observed in purine bases. The remaining conformers adopt a *syn* conformation. The conformational search of $H(dGMP)^{2-}$ yielded 5 *anti* and 2 *syn* conformations, the *syn* conformer being the most stable one (Fig. 5c). The *anti* conformation became the most stable form of $H_2(dGMP)^-$. It is worth mentioning that, for the latter species, only 2 *anti* conformations were found, whereas 8 other conformers adopted a

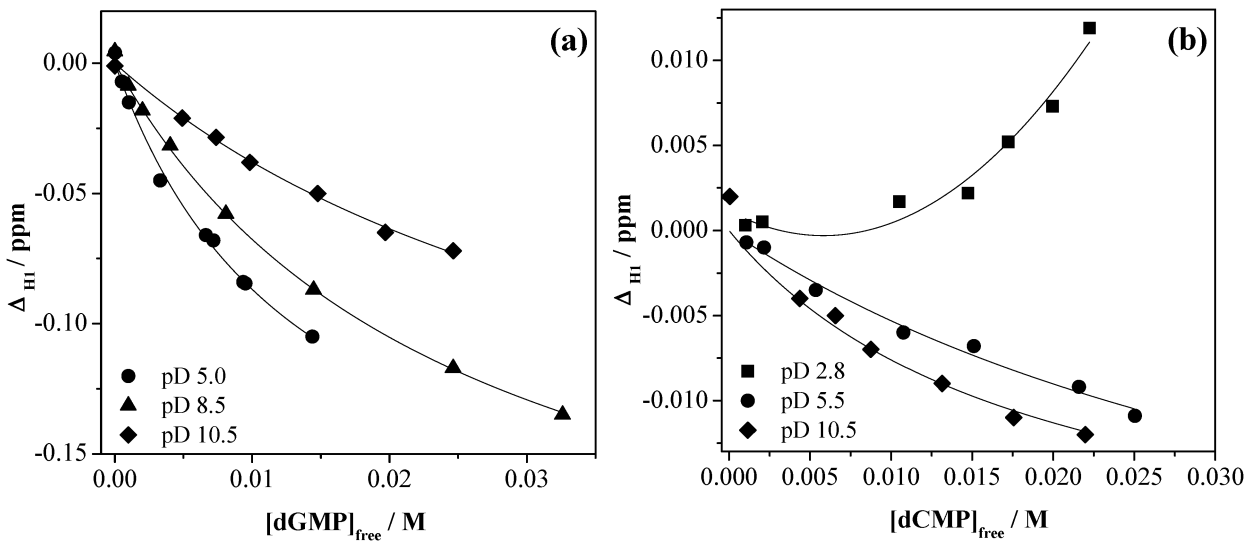

Fig. 4 Chemical shift ($\Delta = \delta_{obs} - \delta_0$) of the norharmane C1–H signal as a function of free (a) dGMP and (b) dCMP concentration.

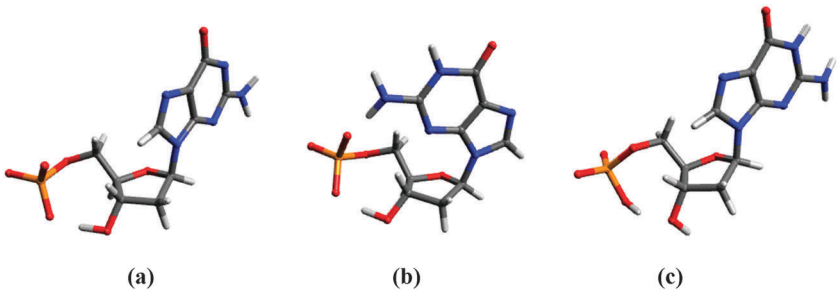

Fig. 5 The most stable nucleotide conformations for (a) $(dGMP)^{3-}$, (b) $H(dGMP)^{2-}$ and (c) $H_2(dGMP)^{-}$.

syn conformation. Fig. 5 shows the most stable conformers found for each dGMP species.

For $(dCMP)^{2-}$, the conformational search led to 16 *anti* conformations, within the energy window of 2 kcal mol^{-1}. All these conformations show that the N1–C6 bond projected onto or near the sugar ring. No *syn* conformations were found. The lowest energy form for $H(dCMP)^{-}$ was found to be an *anti* conformation. Other 14 *anti* conformers, as well as 6 *syn* conformations, were also found. Likewise, 12 conformers were found for $H_2(dCMP)^{\pm}$ within the energy penalty of 2 kcal mol^{-1}, 8 of them showing an *anti* conformation and the remaining 4 in a *syn* conformation. It is worth mentioning that the most stable conformer found for each dCMP acid–base species adopts an *anti* conformation, as depicted in Fig. 6.

In the case of norharmane–dGMP and norharmane–dCMP complexes, the conformational search using genetic algorithms led to several hundred conformers for the G5.0, G8.5 and G10.5 systems, on the one hand, and for the C2.8, C5.5 and C10.5 systems, on the other hand. All those conformers were further optimized at the PM6-DH+ level of theory. As in isolated molecules, those complexes presenting a HOF up to 2 kcal mol^{-1} above the lowest energy conformer were considered to obtain a statistically averaged HOF for each system. Thus, an approach to the intermolecular interaction enthalpy is given by subtracting the HOFs of nucleotides and norharmane species from the HOF of the complex. Fig. 7 shows the molecular structure of the lowest energy conformer for each complex together with their statistically averaged HOF values. It can be seen that calculated HOFs are in reasonable agreement with experimental binding constants. The averaged values of binding constants for the corresponding systems displayed in Tables 1 and 3 suggest that the entropic term $T\Delta S$ must be negative for all the cases, which means that the complexation process leads to highly ordered systems. Besides, a parallel π-stacking interaction is observed in almost all the systems. System C2.8 is the only exception as no π-stacking between the norharmane and the nucleobase rings is observed (Fig. 7d). This finding is in good agreement with the NMR results shown above (Fig. 4b). In addition, different types of hydrogen bonds can be seen for all conformations, too. Geometric parameters that define the hydrogen bonding interaction for each conformation are included in ESI† (Tables S2 and S3).

Fluorescence emission spectroscopy: The deactivation of norharmane fluorescence emission by the dNMPs was analyzed, under different pH conditions. These data supported the results obtained from UV-vis and RMN ^1H spectroscopy studies regarding the interaction of these molecules in their ground states and also provided useful information about the interaction between S_1 of norharmane and dNMPs in their ground states. Data recorded in norharmane–dGMP systems (G5.0, G8.5 and G10.5) are presented in Fig. 8, as a typical example among the 9 cases investigated. Data for norharmane–dCMP systems are shown in ESI† (Fig. S4 to S7).

For all the investigated cases, despite that the fluorescence intensity of norharmane showed a strong decrease with the increase of dNMP concentration, the wavelength of the emission maximum remained unchanged. Moreover, in the whole pH-range investigated, no additional emission bands were observed (see the normalized emission spectra shown in the insets in the left column of Fig. 8). This fact indicates that, as a consequence of the interaction, no new emitting species are generated: neither emitting complexes nor protonated/deprotonated norharmane excited species. It is also worth mentioning that in alkaline pH conditions, where the neutral

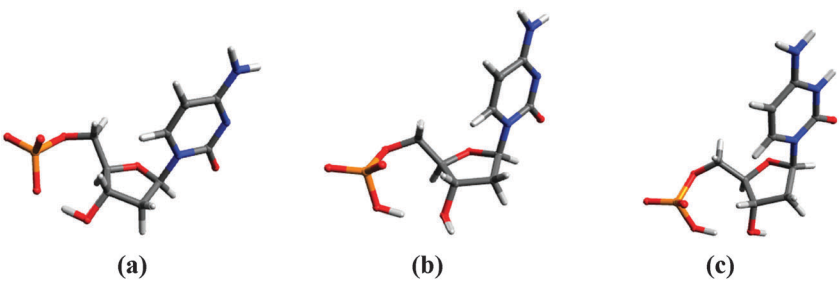

Fig. 6 The most stable nucleotide conformations for (a) $(dCMP)^{2-}$, (b) $H(dCMP)^{-}$ and (c) $H_2(dCMP)^{\pm}$.

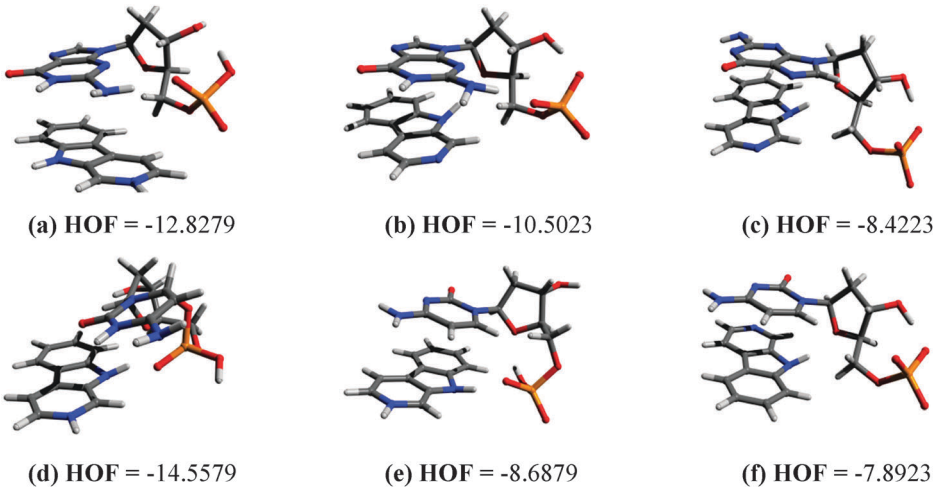

Fig. 7 The lowest energy conformation and heat of formation (HOF, in kcal mol^{-1}) for the six complexes investigated in this work: (a) G5.0, (b) G8.5, (c) G10.5, (d) C2.8, (e) C5.5 and (f) C10.5.

form of norharmane (nHo) is the predominant species in the ground state, such a decrease is only observed in the emission band centered at ~450 nm (*i.e.*, the fluorescence emission band assigned to the protonated excited species of norharmane, $^1[nHoH^+]^*$),[15] whereas the band centered at ~380 nm (assigned to the neutral norharmane species) remains unchanged. This fact suggests that $^1[nHoH^+]^*$ is the main excited species involved in the interaction processes.

In time-resolved experiments, first-order kinetics were observed for all fluorescence decays of norharmane in the presence of different concentrations of nucleotides. Except for systems A2.5 and A5.4 (see discussion below), the corresponding fluorescence lifetimes (τ_F) decreased as a function of nucleotide concentration. Typical traces obtained for the quenching of fluorescence of norharmane by dGMP are shown in Fig. 8 (right column).

In order to discern whether the nature of the interaction is static and/or dynamic, comparative Stern–Volmer plots were depicted from steady-state and time-resolved experiments (*i.e.*, I_F^0/I_F and τ_F^0/τ_F, respectively). Data showed that, except for the case of systems A2.5 and A5.4, where a purely static quenching took place (see below), all the other systems showed the same trend, *i.e.*, a non-linear Stern–Volmer behavior in the decrease of I_F as a function of dNMP concentration. In contrast, the dependence of τ_F^0/τ_F on dNMP concentration was linear, with a positive slope. Interestingly, the dynamic and static contributions to the overall fluorescence quenching observed strongly depend on the nature of the nucleobase and also on the pH. The main conclusions drawn from this analysis can be summarized as follows:

(i) Comparison of the binding constant values calculated from fluorescence steady-state (K_{SS}) and UV-vis (K_{G1}) or ^{1}H-NMR (K_{G2}) studies reveals that there are no significant differences between these three groups of experimental data (Table 1). Thus, in the whole pH-range investigated, norharmane forms static complexes in its electronic ground state with all the dNMP investigated (C2.8 represents an exception, see discussion below).

(ii) For the three norharmane–dGMP systems studied (G5.0, G8.5 and G10.5), the decrease of the integrated fluorescence intensity as a function of nucleotide concentration showed non-linear Stern–Volmer behavior that could be fitted with eqn (4). In addition, the dependence of τ_F^0/τ_F on dGMP concentration was linear, with a positive slope different from zero (insets of Fig. 8). The values reported in Table 1 suggest that although a combination of both dynamic and static quenching is observed, under alkaline conditions (G8.5 and G10.5) dynamic prevails over the static contribution, whereas under acidic conditions (G5.0), both quenching mechanisms equally contribute.

Based on the corresponding quenching constant values (K_D and K_{SS}), listed in Table 1, we can conclude that the static interaction decreases as the negative charge on the dGMP molecule increases (*i.e.*, $K_{SS}^{G5.0} > K_{SS}^{G8.5} > K_{SS}^{G10.5}$). This trend is in agreement with the results obtained from UV-vis spectroscopy and ^{1}H RMN analysis. In contrast, the dynamic interaction increases in the opposite direction (*i.e.*, $K_D^{G5.0} < K_D^{G8.5} < K_D^{G10.5}$).

(iii) Although dAMP is also a purine nucleotide, the results described in the previous paragraph are quite different from those described previously for the norharmane–dAMP system.[6] Our studies revealed that under acidic conditions (A2.5 and A5.4), where $nHoH^+$ is present, the first singlet excited state of the protonated norharmane ($^1[nHoH^+]^*$) is deactivated by dAMP *via* a purely static process, whereas in alkaline media (A10.5) the dynamic contribution dominates the deactivation process.[6]

(iv) In the case of dCMP the quenching observed was quite minor (Fig. S4 and S5 in ESI†). Under alkaline conditions (C10.5), this pyrimidine nucleotide showed a pure dynamic contribution to the total S_1 deactivation (Fig. S6 in ESI†). Thus, under this pH condition, no association between $(dCMP)^{2-}$ and nHo in its ground state occurs, in the whole concentration range analyzed.

In contrast, under acidic conditions (C2.8 and C5.5), the total deactivation observed was rather small, with a contribution of both static and dynamic quenching. The small K_{SS} values observed (Table 3) are in agreement with the non-measurable or negligible

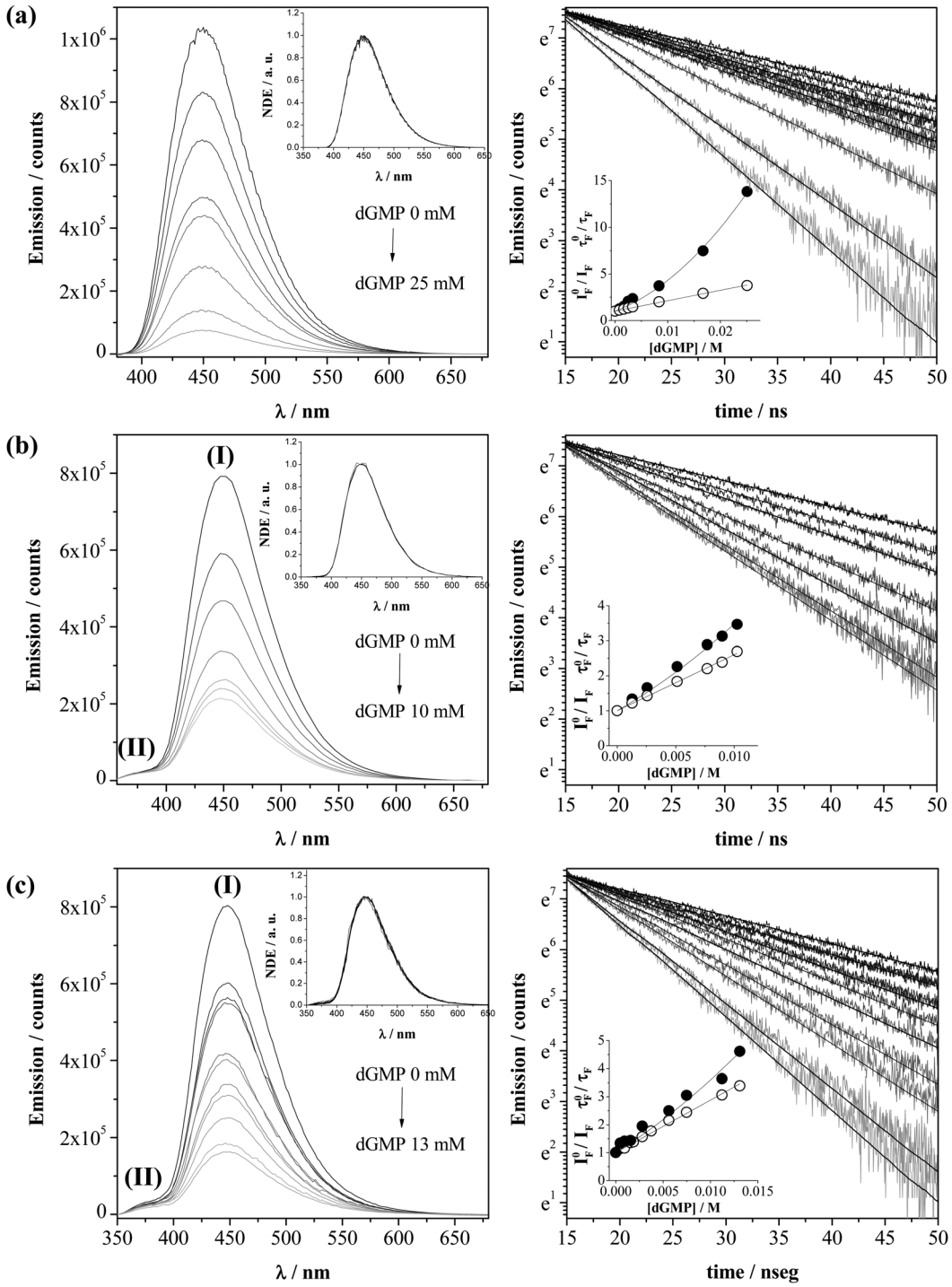

Fig. 8 Corrected fluorescence spectra (left column) and fluorescence decays (right column) of norharmane emission in aqueous solution (20 μM) in the absence and in the presence of increasing amounts of dGMP. The variation in dGMP concentration (mM) appears above each spectrum. Insets in the left column: normalized emission (NE) spectra. (I) and (II) correspond to the emission bands of $nHoH^+$ and nHo, respectively. Insets in the right column: Stern–Volmer plots of fluorescence intensities and lifetimes (I_F, black circles; τ_F, white circles). (a) pH 5.0, (b) pH 8.5 and (c) pH 10.5.

K_G values observed by UV-vis and ^{1}H-NMR spectroscopy. Thus, the interaction between norharmane and dCMP in their ground states is quite weak taking place only under acidic conditions where $nHoH^+$ is present (*i.e.*, C2.8 and C5.5).

Taking into account the fact that UV-vis and ^{1}H-NMR spectroscopy showed a rather weak π-stacking interaction between norharmane and cytidine, the electrostatic attraction between the positive net charge of the protonated pyrimidine-nitrogen present in the norharmane moiety and the negative charge localized in the phosphate group of the nucleotide should, therefore, dominate the interaction mode.

(v) For the experiments performed in alkaline media where the nHo is predominant (G8.5, G10.5, A10.5 and C10.5), the three nucleotides exhibited similar K_D values, showing that dynamic quenching of the singlet excited state of norharmane is not influenced by the nature of the nucleobase. Under these pH conditions, K_{SS} values (Tables 1 to 3) are rather low (or null in the case of C10.5). Thus, only ground state complexes between nHo and purine nucleotides can be formed but the formation of the corresponding hetero-complexes will be significant only at relatively high reactant concentrations. K_{SS} values are the same, within the experimental error, as those obtained from the UV-vis and ^{1}H-NMR spectroscopy. The latter fact reveals that, in alkaline solution, nHo is involved in the ground state static complexation (*i.e.*, no exciplex between $^1[nHoH^+]^*$ and dNMPs is formed).

(vi) Under acidic conditions (G5.0, A2.5, A5.4, C2.8 and C5.5), the three nucleotides showed a dominant static contribution to the overall $nHoH^+$ fluorescence quenching. The capability of $nHoH^+$ to form complexes with nucleotides strongly depends on the chemical nature of the nucleobase: its interaction with purine nucleotides is larger than that observed with pyrimidine nucleotides, under the same experimental conditions. This could be due to the fact that both purines and $nHoH^+$ have polycyclic structures leading to a stronger π-stacking interaction than that observed with dCMP, a monocyclic structure.

(vii) For those systems where a dynamic contribution was detected, a bimolecular quenching rate constant (k_q) could be calculated from K_D values, $k_q = K_D\tau_F^0$ (see Tables 1–3). For all the cases, k_q values are under the diffusion-controlled limits and are quite similar to those reported in the literature for related compounds.[6,51]

Comparison of k_q values listed in Tables 1–3 shows that the overall deactivation is much more efficient in alkaline than in acidic media, where k_q are extremely low or null. Upon excitation, even at pH 10.5, $^1[nHoH^+]^*$ is the predominant species.[7] Thus, $^1[nHoH^+]^*$ is the electronic excited species that is involved in the dynamic quenching observed.[52] Moreover, our results indicate that the nature of the nucleobase does not affect much the kinetic of the deactivation process. Certainly, k_q values reported herein for G8.5, G10.5, A10.5 and C10.5 are quite close to k_q reported for the fluorescence quenching of harmane by phosphate anions[21] (*i.e.*, 9.7×10^9 M^{-1} s^{-1}, measured in NH_3–NH_4Cl pH 8.7 buffer solutions; see footnotes of Tables 1–3). Balón *et al.*[21] suggested that the dynamic component observed for a related βC is due to a proton transfer reaction between the excited state of the βC cations and the phosphate group of the mononucleotide. However, our results

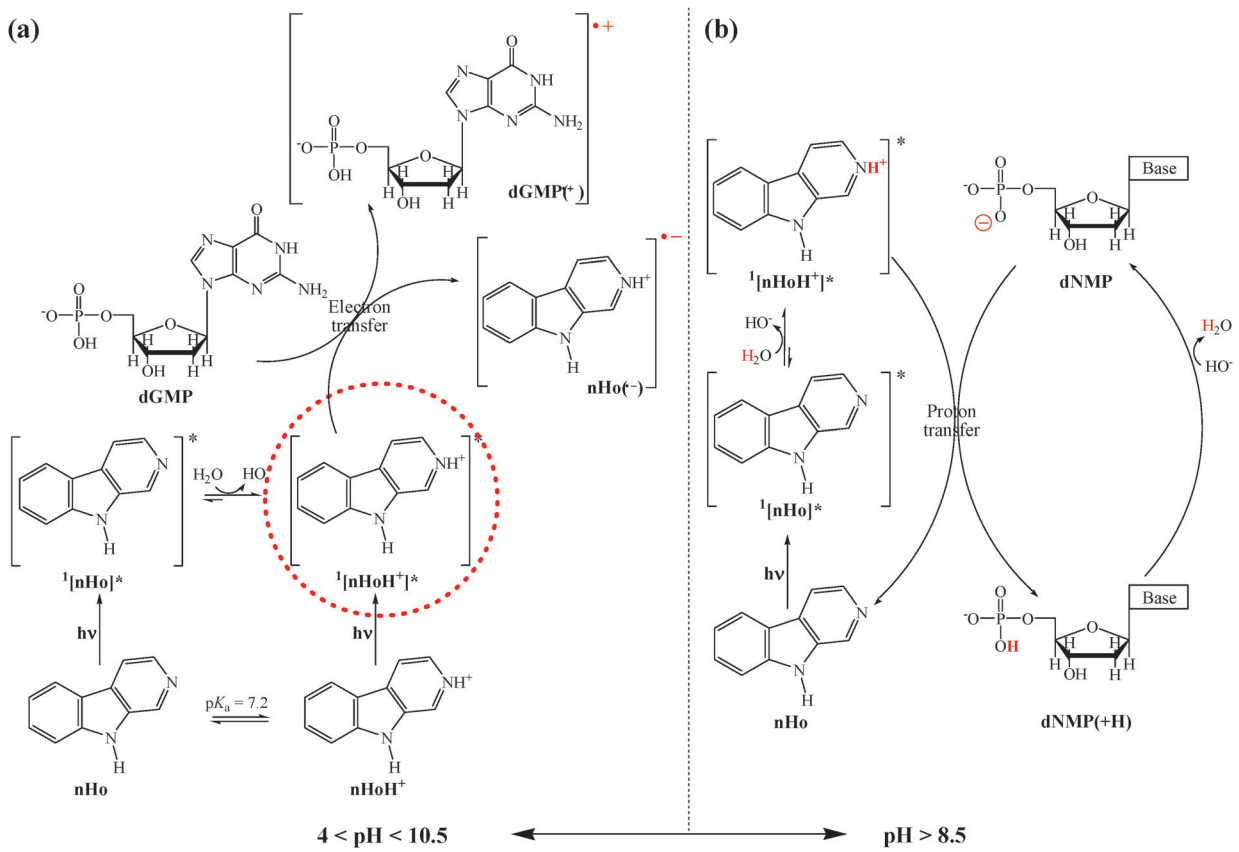

Scheme 2 Mechanisms suggested for the dynamic quenching process operating in (a) the whole pH range investigated where an electron transfer mechanism takes place between excited norharmane and dGMP. In order to make things easier only $dGMP^-$ is depicted. However, in the whole pH range, other species might be present; (b) alkaline pH conditions where a proton transfer mechanism operates for the three nucleotides investigated (dNMP = dGMP, dAMP or dCMP).

indicate that such a process would only take place under alkaline conditions, where the phosphate group of the nucleotide is completely deprotonated, even the less acidic oxygen with a $pK_a \sim 6$.

It is noteworthy that in the case of dGMP at pH 8.5 and 10.5, the dynamic deactivation is even faster than that observed for the other nucleotides (k_q values are slightly higher). This fact would indicate the presence of additional deactivation pathways. Such pathways could be related to additional photochemical processes that yield dGMP photooxidation. As a proof of principle, we have investigated the comparative damage on the three investigated dNMPs photosensitized by norharmane (Fig. S8 in ESI†). Clearly, dGMP is the most photosensitive target, whereas no photosensitized degradation was observed in dCMP. The damage observed for dAMP was quite small and it was already demonstrated that it takes place from the static hetero-complex.[6] This photochemical reactivity agrees with the fluorescence quenching trend observed above.

On the basis of the global analysis of all the results presented in this work, two different mechanisms are able to explain the distinctive dynamic deactivation observed for the three nucleotides in the whole pH conditions investigated, as shown in Scheme 2: (a) a process that takes place only under alkaline conditions, involving a proton transfer from S_1 of the protonated norharmane ($^1[nHoH^+]^*$) to the oxygen in the phosphate group of dNMPs (Scheme 2b) and (b) a second mechanism involving an electron transfer reaction from $^1[nHoH^+]^*$ to the guanine base (Scheme 2a).

Conclusions

In this work, the effect of pH on the interaction between norharmane and deoxynucleotides has been investigated. The findings described in this manuscript allow us to underline that (i) the type and extent of the interaction of βC and deoxynucleotides, in both ground and excited electronic states, as well as the photochemical, photophysical and spectroscopic behavior of both free and bound βC (*i.e.*, as part of the βC–dNMP complex), clearly depend on the molecular structure of the nucleobase and the pH. This is an important point to keep in mind when considering the roles played by βCs in natural systems. (ii) Spectroscopic data as well as chemometric analysis reveal that complex formation between norharmane and purine nucleotides leads to a shift towards higher pH values of the apparent pK_a for bound norharmane relative to free norharmane. This observation may provide important insights into features that facilitate the binding of βCs and biomolecules and, in turn, contribute to a better understanding of photosensitized processes where these alkaloids play a key role. It is worth mentioning that the damage on biomolecules photosensitized by βCs strongly depends on the strength of the interaction: the strongest the interaction, the highest the photosensitizing activity of these alkaloids.

Data presented show that studies of the effect of pH on the interaction of β-carboline alkaloids and deoxynucleotides, in aqueous media, provide a good opportunity to examine a variety of fundamental physicochemical phenomena. Moreover, a deep knowledge of the molecular basis of the interaction between organic molecules of biological importance not only provides relevant information to further elucidate the roles played by these compounds in a range of biological systems, but also provides relevant information in other fields of chemistry and technology where the packing and co-assembly of hetero-aromatic rings play a key role.

Acknowledgements

The present work was partially supported by CONICET (PIP 11220120100072CO), ANPCyT (PICT 2012-0423 and 2012-0888) and UBA (X088) and UNSAM (E103). MMG thanks CONICET for postdoctoral research fellowships. MMG, MPD, RPD, FSGE, REB and FMC are research members of CONICET. FMC thanks DAAD for the spectrofluorometer Fluoromax4-HORIBA provided in the framework of Equipment Grants for Higher Education and Comparable Scientific and Research Institutions in Developing Countries.

Notes and references

1 T. Mori, A. Nakagawa, N. Kobayashi, M. W. Hashimoto, K. Wakabayashi, K. Shimoi and N. Kinae, *J. Radiat. Res.*, 1998, **39**, 21–33.
2 K. Shimoi, H. Kawabata and I. Tomita, *Mutat. Res., Fundam. Mol. Mech. Mutagen.*, 1992, **268**, 287–295.
3 M. M. Gonzalez, M. Pellon-Maison, M. A. Ales-Gandolfo, M. R. Gonzalez-Baró, R. Erra-Balsells and F. M. Cabrerizo, *Org. Biomol. Chem.*, 2010, **8**, 2543–2552.
4 M. M. Gonzalez, M. Vignoni, M. Pellon-Maison, M. A. Ales-Gandolfo, M. R. Gonzalez-Baro, R. Erra-Balsells, B. Epe and F. M. Cabrerizo, *Org. Biomol. Chem.*, 2012, **10**, 1807–1819.
5 M. Vignoni, F. A. O. Rasse-Suriani, K. Butzbach, R. Erra-Balsells, B. Epe and F. M. Cabrerizo, *Org. Biomol. Chem.*, 2013, **11**, 5300–5309.
6 M. M. Gonzalez, F. A. O. Rasse-Suriani, C. A. Franca, R. Pis Diez, Y. Gholipour, H. Nonami, R. Erra-Balsells and F. M. Cabrerizo, *Org. Biomol. Chem.*, 2012, **10**, 9359–9372.
7 M. M. Gonzalez, J. Arnbjerg, M. Paula Denofrio, R. Erra-Balsells, P. R. Ogilby and F. M. Cabrerizo, *J. Phys. Chem. A*, 2009, **113**, 6648–6656.
8 M. M. Gonzalez, M. L. Salum, Y. Gholipour, F. M. Cabrerizo and R. Erra-Balsells, *Photochem. Photobiol. Sci.*, 2009, **8**, 1139–1149.
9 F. M. Cabrerizo, J. Arnbjerg, M. P. Denofrio, R. Erra-Balsells and P. R. Ogilby, *ChemPhysChem*, 2010, **11**, 796–798.
10 A. P. Varela, H. D. Burrows, P. Douglas and M. da Graça Miguel, *J. Photochem. Photobiol., A*, 2001, **146**, 29–36.
11 M. J. Tapia, D. Reyman, M. H. Viñas, A. Arroyo and J. M. L. Poyato, *J. Photochem. Photobiol., A*, 2003, **156**, 1–7.
12 M. Krishnamurthy and S. K. Dogra, *J. Chem. Soc., Perkin Trans. 2*, 1986, 1247–1251.
13 A. O. Torrent, F. T. Vert, I. Z. Sanchez and P. M. Casamayor, *J. Photochem.*, 1987, **37**, 109–116.

14 S. Draxler and M. E. Lippitsch, *J. Phys. Chem.*, 1993, **97**, 11493–11496.
15 R. Sakurovs and K. P. Ghiggino, *J. Photochem.*, 1982, **18**, 1–8.
16 K. P. Ghiggino, P. F. Skilton and P. J. Thistlethwaite, *J. Photochem.*, 1985, **31**, 113–121.
17 O. S. Wolfbeis, E. Fürlinger and R. Wintersteiger, *Monatsh. Chem.*, 1982, **113**, 509–517.
18 F. Tomas Vert, I. Zabala Sanchez and A. Olba Torrent, *J. Photochem.*, 1983, **23**, 355–368.
19 F. Tomas Vert, I. Zabala Sanchez and A. Olba Torrent, *J. Photochem.*, 1984, **26**, 285–294.
20 M. L. Alomar, M. M. Gonzalez, R. Erra-Balsells and F. M. Cabrerizo, *J. Photochem. Photobiol., B*, 2014, 26–27.
21 M. Balón, M. A. Muñoz, C. Carmona, P. Guardado and M. Galán, *Biophys. Chem.*, 1999, **80**, 41–52.
22 I. X. García-Zubiri, H. D. Burrows, J. S. Seixas De Melo, M. Monteserín, A. Arroyo and M. J. Tapia, *J. Fluoresc.*, 2008, **18**, 961–972.
23 Z. Miskolczy, M. Megyesi, L. Biczók and H. Görner, *Photochem. Photobiol. Sci.*, 2011, **10**, 592–600.
24 B. S. Kim and J. Y. Lee, *Org. Electron.*, 2013, **14**, 3024–3029.
25 C. W. Lee, Y. Im, J.-A. Seo and J. Y. Lee, *Org. Electron.*, 2013, **14**, 2687–2691.
26 E. D. Glowacki, M. Irimia-Vladu, S. Bauer and N. S. Sariciftci, *J. Mater. Chem. B*, 2013, **1**, 3742–3753.
27 S. S. Danyluk, *Biochemistry*, 1968, **7**, 1038–1043.
28 D. Reyman, M. H. Viñas, G. Tardajos and E. Mazario, *J. Phys. Chem. A*, 2012, **116**, 207–214.
29 Norharmane is a good model compound for aromatic βCs in general due to its chemical structure (see Fig. 1). All full aromatic βCs possess a norharmane-like skeleton moiety, and the difference between them is the nature and position of the substituents.
30 P. Salomaa, L. L. Schaleger and F. A. Long, *J. Am. Chem. Soc.*, 1964, **86**, 1–7.
31 F. García Einschlag, *Kinesim, v. 9.5, multipurpose program for kinetics and photochemistry (Copyright No. 395814)*, INIFTA, Argentina, 2005.
32 C. Ruckebusch, S. Aloïse, L. Blanchet, J. P. Huvenne and G. Buntinx, *Chemom. Intell. Lab. Syst.*, 2008, **91**, 17–27.
33 R. Tauler, *Chemom. Intell. Lab. Syst.*, 1995, **30**, 133–146.
34 M. Goez and I. Sartorius, *J. Am. Chem. Soc.*, 1993, **115**, 11123–11133.
35 M. Blanco, A. C. Peinado and J. Mas, *Anal. Chim. Acta*, 2005, **544**, 199–205.
36 M. Meloun, J. Čapek, P. Mikšík and R. G. Brereton, *Anal. Chim. Acta*, 2000, **423**, 51–68.
37 A. de Juan and R. Tauler, *Anal. Chim. Acta*, 2003, **500**, 195–210.
38 P. J. Gemperline and E. Cash, *Anal. Chem.*, 2003, **75**, 4236–4243.
39 M. Garrido, I. Lázaro, M. S. Larrechi and F. X. Rius, *Anal. Chim. Acta*, 2004, **515**, 65–73.
40 Note that the lowest detection limit of our fluorescence set-up is 100 ps. Therefore, emitting species with lifetimes shorter than the above limit cannot be detected.
41 J. Reuben, *J. Am. Chem. Soc.*, 1973, **95**, 3534–3540.
42 E. Gaggelli, N. D'Amelio, N. Gaggelli and G. Valensin, *Eur. J. Inorg. Chem.*, 2000, 1699–1706.
43 M. J. Vainio and M. S. Johnson, *J. Chem. Inf. Model.*, 2007, **47**, 2462–2474.
44 MOPAC2009, J. J. P. Stewart, *Stewart Computational Chemistry*, Colorado Springs, CO, USA, 2008, http://OpenMOPAC.net.
45 C. Carmona, M. Galan, G. Angulo, M. A. Munoz, P. Guardado and M. Balon, *Phys. Chem. Chem. Phys.*, 2000, **2**, 5076–5083.
46 Despite the concept of π-stacking is still controversial and a more general expression would be ''non-covalent dispersion interaction'', taking into account the results of section ''Molecular modeling'', we will refer to it as π-stacking.
47 Results obtained for norharmane–dAMP system are shown with comparative purpose, and were already published ref. 6.
48 K. J. Neurohr and H. H. Mantsch, *Can. J. Chem.*, 1979, **57**, 1986–1994.
49 R. Tribolet and H. Sigel, *Biophys. Chem.*, 1987, **27**, 119–130.
50 S. Grimme, *Angew. Chem., Int. Ed.*, 2008, **47**, 3430–3434.
51 G. Petroselli, M. L. Dántola, F. M. Cabrerizo, C. Lorente, A. M. Braun, E. Oliveros and A. H. Thomas, *J. Phys. Chem. A*, 2009, **113**, 1794–1799.
52 Note the fast protonation of the excited stated of the neutral form that takes place in aqueous environments.